Title

A personal glucose meter-utilized strategy for portable and label-free detection of hydrogen peroxide

Authors

Lee, Sangmo
Kim, Hyoyong
Yoon, Junhyeok
et al.

Publication Date

2024-06-01

DOI

10.1016/j.bios.2024.116141

Biosensors and Bioelectronics 253 (2024) 116141

Contents lists available at ScienceDirect

Biosensors and Bioelectronics

journal homepage: www.elsevier.com/locate/bios

A personal glucose meter-utilized strategy for portable and label-free detection of hydrogen peroxide

Sangmo Lee [1], Hyoyong Kim [1], Junhyeok Yoon, Yong Ju, Hyun Gyu Park [*]

Department of Chemical and Biomolecular Engineering (BK21 Four), Korea Advanced Institute of Science and Technology (KAIST), 291 Daehak-ro, Yuseong-gu, Daejeon, 34141, Republic of Korea

A R T I C L E I N F O

Keywords:
Personal glucose meter
Hydrogen peroxide
Choline
Horseradish peroxidase
Ferri/ferrocyanide

A B S T R A C T

Rapid and precise detection of hydrogen peroxide (H_2O_2) holds great significance since it is linked to numerous physiological and inorganic catalytic processes. We herein developed a label-free and washing-free strategy to detect H_2O_2 by employing a hand-held personal glucose meter (PGM) as a signal readout device. By focusing on the fact that the reduced redox mediator ($[Fe(CN)_6]^{4-}$) itself is responsible for the final PGM signal, we developed a new PGM-based strategy to detect H_2O_2 by utilizing the target H_2O_2-mediated oxidation of $[Fe(CN)_6]^{4-}$ to $[Fe(CN)_6]^{3-}$ in the presence of horseradish peroxidase (HRP) and monitoring the reduced PGM signal in response to the target amount. Based on this straightforward and facile design principle, H_2O_2 was successfully determined down to 3.63 μM with high specificity against various non-target molecules. We further demonstrated that this strategy could be expanded to identify another model target choline by detecting H_2O_2 produced through its oxidation promoted by choline oxidase. Moreover, we verified its practical applicability by reliably determining extracellular H_2O_2 released from the breast cancer cell line, MDA-MB-231. This work could evolve into versatile PGM-based platform technology to identify various non-glucose target molecules by employing their corresponding oxidase enzymes, greatly advancing the portable biosensing technologies.

1. Introduction

Hydrogen peroxide (H_2O_2), a non-radical reactive oxygen species, is produced as a short-lived product in numerous biological processes and inorganic catalytic processes (Gough and Cotter, 2011; Groeger et al., 2009; Mahdi et al., 2022; Meitzler et al., 2019; Yousefi et al. 2016, 2017, 2019a, 2019b, 2021a, 2021b, 2021c). Particularly, it is well known that H_2O_2 plays important roles in host defense and various oxidative biosynthetic reactions. In recent years, it has also been of great importance due to its pivotal role in the cellular signal transductions involved in diverse cellular processes such as proliferation, differentiation, and motility (D'Autréaux and Toledano, 2007; Forman, 2007; Janssen-Heininger et al., 2008; Purohit et al., 2019; Rhee, 2006; Stone and Yang, 2006; Tanner et al., 2011; Veal et al., 2007). For instance, H_2O_2 binds to cysteine residue within the active site of protein tyrosine phosphatase (PTP), a crucial regulator of cellular signal transduction, and serves as a critical factor for the sophisticated regulation of the signal transductions associated with cell growth, metabolic homeostasis, and neural transmission (Andersen et al., 2004; Garcia and Carroll, 2014; Östman et al., 2011). As a consequence, a higher H_2O_2 level than the normal concentration might cause permanent damage to PTP, which is deeply associated with various diseases such as Alzheimer's disease, Parkinson's disease, and cancer (Brand, 2016; Machado et al., 2017; Meng and Zhang, 2013). It is also well established that oxidative stress induced by H_2O_2 is an important cause of cell damage linked to the initiation and progression of numerous human diseases (Meitzler et al., 2019; Rhee, 2006; Stone and Yang, 2006). Moreover, H_2O_2 has been reported to be closely linked to the distinctive features of cancer cells such as their altered metabolism (Sullivan et al., 2016), dysfunctional mitochondria (Boland et al., 2013; Kim et al., 2006; Srinivasan et al., 2017), or increased ROS production processes (Panieri and Santoro, 2016), and the identification of H_2O_2 from cancer cells has attracted considerable attention (Asif et al., 2017; Mohammadniaei et al., 2018; Ren et al., 2021).

Due to these clinical significances, several assay kits have been developed and successfully commercialized to determine H_2O_2 in biological samples such as serum, plasma, and urine (Mohanty et al., 1997; Summers et al., 2013; Wang et al., 2017). They mainly rely on the

* Corresponding author.
E-mail address: hgpark@kaist.ac.kr (H.G. Park).
[1] These authors equally contributed to this work.

https://doi.org/10.1016/j.bios.2024.116141
Received 10 December 2023; Received in revised form 31 January 2024; Accepted 17 February 2024
Available online 19 February 2024

horseradish peroxidase (HRP)-promoted oxidation of the signaling molecules, which would result in the oxidized products generating either fluorescent, luminescent, or colorimetric signals in response to H_2O_2. They are capable of reliably quantifying the H_2O_2 level but normally require bulky and costly instruments for signal acquisition and interpretation, significantly limiting their wide-spread applications in facility-limited environments.

Meanwhile, a personal glucose meter (PGM) has emerged as a compelling alternative signal readout device for the realization of point-of-care (POC) testing for non-glucose analytes, and during the past decade, it has been extensively utilized to construct various biosensing systems by transducing the concentrations of target analytes of interest into the PGM signals (Ahn et al. 2018, 2019; Fang et al., 2018; Kim et al. 2020a, 2020b, 2020c, 2020d; Lan et al., 2016; Wu et al., 2018; Xiang and Lu, 2011, 2012a, 2012b; Zhang et al., 2020; Zhu et al., 2019). Most representatively, Xiang and Lu, 2011 developed PGM-based strategies to identify various non-glucose targets such as cocaine, adenosine, interferon-gamma of tuberculosis, and uranium by employing an invertase-labeled DNA probe. Our group also successfully developed several novel PGM-based strategies to detect ATP (Ahn et al., 2018), alkaline phosphatase (Ahn et al., 2019), target DNA (Kim et al. 2020a, 2020c), telomerase (Kim et al., 2020b), and terminal transferase (Kim et al., 2020d) by utilizing hexokinase-mediated cascade enzymatic reactions or glucose oxidase-mimicking activity of cerium oxide nanoparticle. The conventional approaches to detect non-glucose analytes on a PGM, yet, mainly relied on specially designed and complicated mechanisms correlating the target analyte with the glucose concentration, which would significantly hinder their expansion as a versatile biomolecule detection platform for various non-glucose target substances.

Afterward, it was focused that the PGM signal is produced exclusively by the final amount of redox mediators, and Zhang et al. (2016) developed a new strategy to detect several non-glucose analytes on a PGM by correlating them directly with the redox mediators without involving glucose. Specifically, they utilized the reduced form of nicotinamide adenine dinucleotide (NADH) capable of reducing the redox mediator to identify the NADH-dependent enzyme and substrate on a PGM. The technique relies on the fact that NADH is either produced or consumed by the target-induced enzymatic reactions, which would accordingly enhance or decrease the reduction of the redox mediator, consequently leading to a change in the final PGM signal according to the concentrations of target analytes. Based on this principle, they successfully identified L-lactate and glucose-6-phosphate dehydrogenase on a PGM. Recently, another research group reported the PGM-based H_2O_2 detection method utilizing acetylthiocholine iodide (Zhang et al., 2022) or ascorbic acid oxidase (AAO) (Tian et al., 2022) to correlate redox mediators with target H_2O_2. They successfully identified H_2O_2 on a PGM, however, those strategies relied on intricate mechanisms which resulted in non-specific response to NaClO or inherent instability arising from short-lived AAO-H_2O_2 intermediate.

Upon this background, we herein developed a simple and label-free method to quantify H_2O_2 on a hand-held PGM without the involvement of glucose molecules. This strategy relies on the target H_2O_2-induced catalysis of HRP to directly oxidize ferrocyanide ($[Fe(CN)_6]^{4-}$) to ferricyanide ($[Fe(CN)_6]^{3-}$), which would decrease the concentration of $[Fe(CN)_6]^{4-}$ in the analyte solution and accordingly decrease the PGM signal. Based on this simple and straightforward design principle, we successfully identified H_2O_2 very rapidly and conveniently, yielding high sensitivity and specificity.

2. Materials and methods

2.1. Materials

Sodium phosphate, tris(hydroxymethyl)aminomethane (Tris), ethylenediaminetetraacetic acid (EDTA), potassium chloride (KCl), potassium ferrocyanide (K_4 $[Fe(CN)_6]\cdot 3H_2O$), choline chloride, sodium chloride (NaCl), magnesium chloride ($MgCl_2$), ammonium chloride (NH_4Cl), phenylalanine, cysteine, tryptophan, horseradish peroxidase (HRP), choline oxidase, human serum, phorbol 12-myristate 13-acetate (PMA), and Peroxide Assay Kit (MAK311) were purchased from Sigma Aldrich (St. Louis, MO, USA). Hydrogen peroxide (H_2O_2) was purchased from Junsei Chemical Co., Ltd. (Chuo-ku, Tokyo, Japan). A personal glucose meter (PGM) was purchased from Green Cross Medical Science Corp. (Yongin-si, Gyeonggi-do, Korea). MDA-MB-231 was obtained from the Korean Cell Line BANK (KCLB). Ultrapure DNase/RNase-free distilled water (DW) purchased from Bioneer® (Daejeon, Korea) was used in all experiments.

2.2. Experimental procedures for H_2O_2 detection

The H_2O_2 detection was conducted in a 20 μL reaction solution containing 9.1 μL DW, 4 μL sodium phosphate buffer (pH 6, 500 mM), 6 μL K_4 $[Fe(CN)_6]\cdot 3H_2O$ (10 mM), 0.5 μL HRP (6 U/mL), and a 0.4 μL analyte solution containing H_2O_2 at varying concentrations. The reaction solution was incubated at room temperature for 2 min, which was then applied on a PGM.

2.3. Experimental procedures for choline detection

For the detection of choline, the choline oxidation reaction was conducted in a 5 μL reaction solution containing 3.5 μL DW, 0.5 μL choline oxidase reaction buffer (10X consisting of 1 M Tris-HCl (pH 8), 0.3 mM EDTA, and 20 mM KCl), 0.5 μL choline oxidase (10 U/mL), and 0.5 μL choline chloride at varying concentrations. The reaction solution was incubated at 40 °C for 60 min. Then, 4.5 μL DW, 4 μL sodium phosphate buffer (pH 6, 500 mM), 6 μL K_4 $[Fe(CN)_6]\cdot 3H_2O$ (10 mM), and 0.5 μL HRP (6 U/mL) were added into the reaction solution, which was then incubated at room temperature for 2 min and applied on a PGM.

2.4. Spike-and-recovery test

2 μL human serum (100%) and 0.4 μL H_2O_2 at varying concentrations were introduced into the premixed reaction solution containing 7.1 μL DW, 4 μL sodium phosphate buffer (pH 6, 500 mM), 6 μL K_4 $[Fe(CN)_6]\cdot 3H_2O$ (10 mM), and 0.5 μL HRP (6 U/mL). The reaction solution was incubated at room temperature for 2 min, which was applied on a PGM. The calibration curve was first constructed from the standard samples containing H_2O_2 at known concentrations and used to determine the H_2O_2 concentrations spiked into the human serum solution.

2.5. Detection of extracellular H_2O_2 released from MDA-MB-231

For the experiments to determine extracellular H_2O_2 released from the cancer cell line, MDA-MB-231 was cultured in DMEM supplemented with 10% FBS under humidified atmosphere containing 5% CO_2 at 37 °C. The cells were then collected during the exponential growth phase in 200 μL of DW at the final concentration of 1×10^7 cell/mL based on cell counting using LUNA-II™ (Logos Biosystems Inc., Gyeonggi-do, Korea). Next, 1 μg/mL PMA was added into the cell suspension and incubated for 5 min, followed by centrifugation at 6000 rpm for 2 min. The supernatant was analyzed by the developed method and the commercial Peroxide Assay Kit (Sigma Aldrich, USA) following the same procedure in section *2.2* and the manufacturer's protocol, respectively.

3. Results and discussion

3.1. The overall principle of the PGM-utilized H_2O_2 detection

In this study, we particularly focused on the fact that $[Fe(CN)_6]^{4-}$

could be directly consumed as a substrate of HRP-promoted oxidation in the presence of H_2O_2 and developed a new facile PGM strategy to detect H_2O_2. As illustrated in Fig. 1, HRP employed in this strategy promote the oxidation reaction of $[Fe(CN)_6]^{4-}$ to $[Fe(CN)_6]^{3-}$ by consuming H_2O_2 as an oxidizing agent. Therefore, the extent of the oxidation reaction increases in proportion to the amount of H_2O_2 in a sample, consequently reducing the amount of $[Fe(CN)_6]^{4-}$ and accordingly decreasing the final PGM signal, while the initial amount of $[Fe(CN)_6]^{4-}$ is just kept unchanged in the negative sample without H_2O_2, maintaining the initial high PGM signal. The reduced amount of the final PGM signal is finally used to quantify H_2O_2.

3.2. Feasibility of the developed strategy

First, we verified the feasibility of the designed principle by investigating the PGM signals obtained from the reaction samples under various combinations of the reaction components. As shown in Fig. 2, the PGM signal was significantly reduced from the original high PGM signal produced by the initial $[Fe(CN)_6]^{4-}$ only when all the reaction components including $[Fe(CN)_6]^{4-}$, HRP, and target H_2O_2 were applied. In the absence of target H_2O_2, on the other hand, the initial PGM signal was almost retained. When HRP was omitted from the reaction, there was no significant change in the PGM signal observed, indicating that the HRP activity was responsible for the promotion of the H_2O_2-induced oxidation of $[Fe(CN)_6]^{4-}$. All these results clearly confirmed that target H_2O_2 would reduce the PGM signal proportionally to its amount and could be quantified according to the mechanism envisioned in the proposed strategy.

3.3. Analytical performance of the developed strategy

To maximize the sensing performance of the developed strategy, we optimized the reaction conditions by examining the degree of PGM signal decrease (D value, defined as $(P_0–P)/P_0$, where P_0 and P are PGM signals obtained from the samples in the absence and presence of H_2O_2, respectively) from the reactions under various conditions. As presented in Fig. S1 and S2, 3 mM $[Fe(CN)_6]^{4-}$ and 150 mU/mL HRP were selected as the optimal conditions and used for further experiments.

We then determined the sensitivity of the developed H_2O_2 detection method by measuring the PGM signals from the reaction samples containing H_2O_2 at varying concentrations. As shown in Fig. 3, the PGM signal properly decreased as the H_2O_2 concentration increased, and the PGM signal showed an excellent linear relationship with the H_2O_2 concentration in the range from 0 to 40 μM ((PGM signal, mg/dL) = -0.3187 (H_2O_2 concentration, μM) + 31.093, $R^2 = 0.9919$), verifying that the developed strategy is capable of reliably quantifying H_2O_2. The limit of detection (LOD) was determined to be 3.63 μM based on the equation, LOD = 3σ/S, where σ is the standard deviation of the PGM signals from the negative control samples without H_2O_2 and S is the slope of the calibration line. The sensitivity of the proposed strategy was quite comparable to or even better than those of previously reported

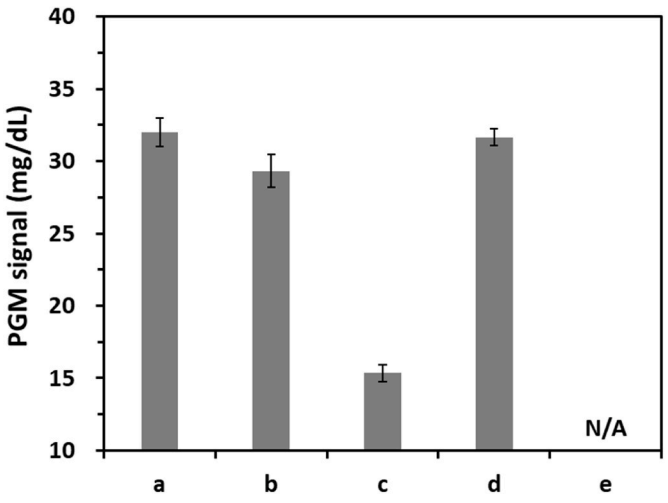

Fig. 2. Feasibility of the PGM-utilized H_2O_2 detection strategy. PGM signals obtained from the samples containing various combinations of the reaction components (a: $[Fe(CN)_6]^{4-}$; b: $[Fe(CN)_6]^{4-}$ + H_2O_2; c: $[Fe(CN)_6]^{4-}$ + H_2O_2 + HRP; d: $[Fe(CN)_6]^{4-}$ + HRP; and e: H_2O_2). The concentrations of $[Fe(CN)_6]^{4-}$, H_2O_2, and HRP were 3 mM, 200 μM, and 150 mU/mL, respectively. Error bars were estimated from triplicate tests.

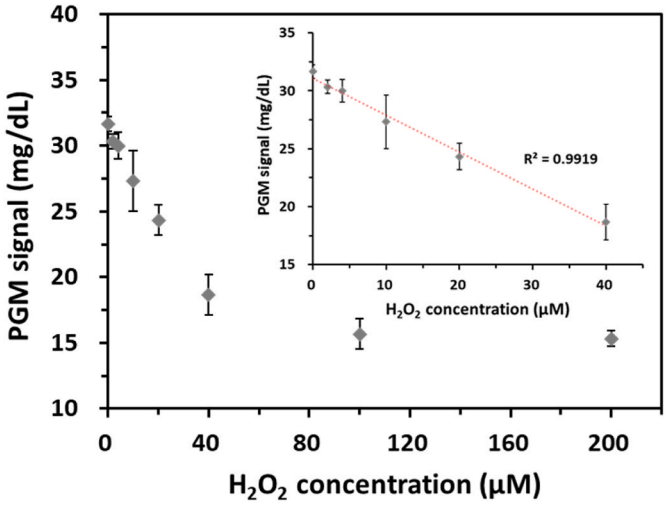

Fig. 3. Sensitivity of the PGM biosensor to identify H_2O_2. PGM signals from the target H_2O_2 at varying concentrations. The inset shows the linear relationship of PGM signals with H_2O_2 concentrations in the range from 0 to 40 μM. The concentrations of $[Fe(CN)_6]^{4-}$ and HRP were 3 mM and 150 mU/mL, respectively. Error bars were estimated from triplicate tests.

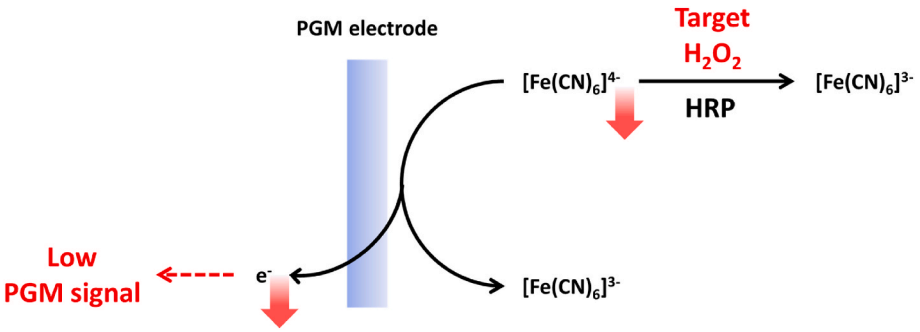

Fig. 1. Schematic illustration of the PGM-utilized strategy to detect H_2O_2 based on the target-induced oxidation of $[Fe(CN)_6]^{4-}$ to $[Fe(CN)_6]^{3-}$.

alternative H_2O_2 detection methods (Table S1). Remarkably, the total assay was very rapidly completed within 3 min and the LOD value was much lower than the typical H_2O_2 concentration in the blood or urine samples obtained from patients with diabetes, coronary artery disease, or chronic renal failure, demonstrating that the designed strategy could be practically applied to the on-site monitoring of the H_2O_2 level in the body fluids (Forman et al., 2016; Kazmierczak et al., 1995; Roberts et al., 2005; Wierusz-Wysocka et al., 1995).

The specificity of this method was next assessed by employing various non-target molecules such as Na^+, Mg^{2+}, NH_4^+, phenylalanine, cysteine, and tryptophan, which are present in human blood and may interfere with the selective detection of H_2O_2 (Tripathi and Chung, 2020). As shown in Fig. 4, the significantly high D value was obtained only from the reaction sample containing H_2O_2, while the other six non-target molecules showed very negligible D values even though they were applied at a 10-fold higher concentration than that of target H_2O_2. These results verified that the developed strategy can specifically identify H_2O_2 against the abundant interfering substances included in the complex biological sample, which is attributed to the well-established design principle utilizing peroxidation reaction of HRP induced by target H_2O_2, directly oxidizing $[Fe(CN)_6]^{4-}$ as a substrate to induce the final signal change.

3.4. Capability of the developed strategy to be expanded to detect various non-glucose target analytes

A wide range of clinically significant biomolecules such as alcohol, galactose, cholesterol, pyruvate, diamine, polyamine, lactate, and choline have the corresponding oxidase enzymes which could promote their oxidations by concomitantly producing H_2O_2 as a byproduct. Therefore, we envisioned that our strategy could be expanded to achieve a new PGM-based platform technology by employing their corresponding oxidase enzymes and monitoring H_2O_2 produced from their oxidations. We selected choline as a model target, which has been reported as a relevant biomarker for several neurodegenerative disorders such as Alzheimer's and Parkinson's diseases (He et al., 2014; Holm et al., 2003; Rahman et al., 2019).

As presented in Fig. 5, the PGM signal gradually decreased with

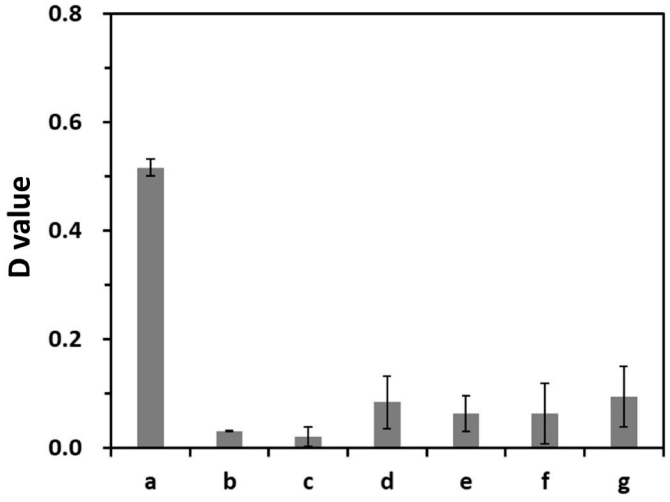

Fig. 4. Specificity of the PGM-utilized H_2O_2 detection strategy. D values in the presence of target and non-target molecules (a: H_2O_2; b: Na^+; c: Mg^{2+}; d: NH_4^+; e: phenylalanine; f: cysteine; and g: tryptophan). The D value is defined as $(P_0–P)/P_0$, where P_0 and P are PGM signals obtained from the samples in the absence and presence of the target or non-target molecule, respectively. The concentrations of $[Fe(CN)_6]^{4-}$, H_2O_2, and HRP were 3 mM, 200 μM, and 150 mU/mL, respectively. The concentrations of non-target molecules were 2 mM (ten-fold higher than that of H_2O_2). Error bars were estimated from triplicate tests.

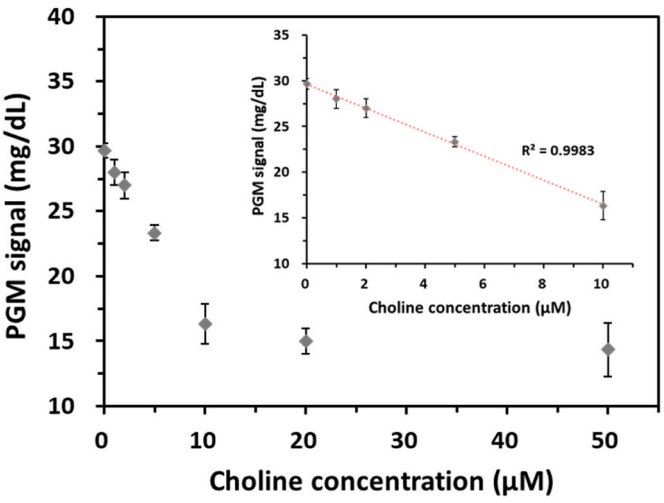

Fig. 5. Sensitivity of the PGM biosensor to identify choline. PGM signals from the target choline at varying concentrations. The inset shows the linear relationship of PGM signals with choline concentrations in the range from 0 to 10 μM. The concentrations of $[Fe(CN)_6]^{4-}$ and choline oxidase were 3 mM and 1 U/mL, respectively. Error bars were estimated from triplicate tests.

increasing choline concentration in the range from 0 to 10 μM with a perfect linear relationship ((PGM signal, mg/dL) = - 1.3129 (choline concentration, μM) + 59.593, R^2 = 0.9983). Notably, the data patterns were almost the same as those from the H_2O_2 target (Fig. 3). The LOD for choline detection was determined to be 1.26 μM, which is quite sensitive enough for the reliable determination of choline included in human blood (Holm et al., 2003). This result demonstrated that the designed strategy could be extensively applied to the detection of various biomolecules by employing their corresponding oxidase enzymes and detecting H_2O_2 produced through the oxidation of the target analytes.

3.5. Practical applicability of the developed strategy

To assess the practical diagnostic capability, we applied this strategy to determine H_2O_2 included in a 10% human serum sample. Since the glucose originally present in human serum might contribute to the PGM signal, we constructed a new calibration curve from the human serum samples spiked with H_2O_2 at varying concentrations. The results in Fig. S3 show that the PGM signal properly decreased as the spiked H_2O_2 concentration increased in the range from 0 to 40 μM ((PGM signal, mg/dL) = - 0.3381 (H_2O_2 concentration, μM) + 39.667, R^2 = 0.9841), and the slope of this calibration curve was almost the same as that from the samples without human serum (Fig. 3), indicating that the efficacy of the target-induced HRP catalysis was rarely influenced by the interfering substances present in human serum. Next, we conducted the spike-and-recovery test based on the obtained calibration curve. As shown in Table S2, this strategy also successfully identified H_2O_2 in the serum samples with great reproducibility and accuracy, as evidenced by the coefficient of variation (CV) less than 10% and the recovery rate between 91 and 106%, respectively.

Afterward, the practical applicability of the developed method was further validated by detecting extracellular H_2O_2 released from the cancer cell line. In this work, we employed MDA-MB-231 as a model which is one of the most representative human breast cancer cell lines and applied phorbol 12-myristate 13-acetate (PMA) to induce the release of H_2O_2 out of the cells (Damianaki et al., 2000; Mohammadniaei et al., 2018; Wu et al., 2011). By following the proposed detection procedures, we determined extracellular H_2O_2 from MDA-MB-231 and compared the result with that from the commercial H_2O_2 assay kit. As shown in Table 1, the concentration of extracellular H_2O_2 released from MDA-MB-231 was determined to be 8.31 μM with excellent

Table 1
Determination of H_2O_2 released from the human breast cancer cell line (MDA-MB-231) using the commercial peroxide assay kit and the proposed PGM-based strategy.

	The commercial peroxide assay kit [a]	This method
Determined H_2O_2 [b] (μM)	7.81 ± 0.34	8.31 ± 0.60
CV [c] (%)	4.35	7.27
Percent agreement [d] (%)	106.40	

[a] The Peroxide Assay Kit (MAK311, Sigma Aldrich, USA) was employed.
[b] Mean ± standard deviation (SD) of triplicate measurements.
[c] Coefficient of variation = SD/Mean × 100.
[d] Percent agreement = H_2O_2 measured using the proposed method/H_2O_2 measured using the commercial Peroxide Assay Kit × 100.

reproducibility with CV less than 10%, and the percent agreement between the two results was 106.4%. All these results confirmed that this strategy could be practically and robustly applied to the detection of target molecules, even in complex and heterogeneous biological samples.

4. Conclusions

We herein developed a facile strategy to conveniently determine H_2O_2 on a hand-held PGM, which relies on the target-induced and HRP-promoted oxidation of $[Fe(CN)_6]^{4-}$ to $[Fe(CN)_6]^{3-}$ followed by the monitoring of the reduced PGM signal due to the consumed $[Fe(CN)_6]^{4-}$. Based on this simple yet compelling detection principle, we successfully determined H_2O_2 down to 3.63 μM and very rapidly within 3 min yielding an excellent discriminating capability against non-target molecules and expanded the strategy to detect the target choline by determining H_2O_2 produced through its oxidation promoted by choline oxidase. Furthermore, we reliably identified extracellular H_2O_2 released from the breast cancer cell line, MDA-MB 231, verifying the practical applicability of the developed strategy. Beyond the conventional approach relying on the correlation of target molecules with glucose in complicated cascade reactions, this work would open a new approach to utilize a more straightforward connection of target analytes with $[Fe(CN)_6]^{4-}$ responsible for the final PGM signal and could evolve into a new PGM-based platform technology to detect diverse biomolecules by employing their corresponding oxidase enzymes.

CRediT authorship contribution statement

Sangmo Lee: Writing – review & editing, Writing – original draft, Validation, Methodology, Investigation, Data curation, Conceptualization. **Hyoyong Kim:** Writing – original draft, Validation, Methodology, Investigation, Data curation, Conceptualization. **Junhyeok Yoon:** Resources, Methodology. **Yong Ju:** Conceptualization. **Hyun Gyu Park:** Writing – review & editing, Writing – original draft, Validation, Supervision, Project administration, Funding acquisition.

Declaration of competing interest

The authors declare that they have no known competing financial interests or personal relationships that could have appeared to influence the work reported in this paper.

Data availability

The data that has been used is confidential.

Acknowledgements

Financial support for this study was provided by the National Research Foundation (NRF) grant funded by the Ministry of Science and ICT (MSIT) of Korea (2022K1A4A8A01080317). This work was also supported by the NRF grant funded by the Korea government (MSIT) (No. RS-2023-00218543) and the Mid-career Researcher Support Program (NRF-2021R1A2B5B03001739) of the NRF.

Appendix A. Supplementary data

Supplementary data to this article can be found online at https://doi.org/10.1016/j.bios.2024.116141.

References

Ahn, J.K., Kim, H.Y., Lee, C.Y., Park, K.S., Park, H.G., 2019. J. Biol. Eng. 13 (1).
Ahn, J.K., Kim, H.Y., Park, K.S., Park, H.G., 2018. Anal. Chem. 90 (19), 11340–11343.
Andersen, J.N., Jansen, P.G., Echwald, S.M., Mortensen, O.H., Fukada, T., Del Vecchio, R., Tonks, N.K., Møller, N.P.H., 2004. FASEB (Fed. Am. Soc. Exp. Biol.) J. 18 (1), 8–30.
Asif, M., Liu, H., Aziz, A., Wang, H., Wang, Z., Ajmal, M., Xiao, F., Liu, H., 2017. Biosens. Bioelectron. 97, 352–359.
Boland, M.L., Chourasia, A.H., Macleod, K.F., 2013. Front. Oncol. 3 (292).
Brand, M.D., 2016. Free Radic. Biol. Med. 100, 14–31.
Damianaki, A., Bakogeorgou, E., Kampa, M., Notas, G., Hatzoglou, A., Panagiotou, S., Gemetzi, C., Kouroumalis, E., Martin, P.-M., Castanas, E., 2000. J. Cell. Biochem. 78 (3), 429–441.
D'Autréaux, B., Toledano, M.B., 2007. Nat. Rev. Mol. Cell Biol. 8 (10), 813–824.
Fang, J., Guo, Y., Yang, Y., Yu, W., Tao, Y., Dai, T., Yuan, C., Xie, G., 2018. Sens. Actuators, B 272, 118–126.
Forman, H.J., 2007. Free Radic. Biol. Med. 42 (7), 926–932.
Forman, H.J., Bernardo, A., Davies, K.J.A., 2016. Arch. Biochem. Biophys. 603, 48–53.
Garcia, F.J., Carroll, K.S., 2014. Eur. J. Med. Chem. 88, 28–33.
Gough, D.R., Cotter, T.G., 2011. Cell Death Dis. 2 (10).
Groeger, G., Quiney, C., Cotter, T.G., 2009. Antioxidants Redox Signal. 11 (11), 2655–2671.
He, S.B., Wu, G.W., Deng, H.H., Liu, A.L., Lin, X.H., Xia, X.H., Chen, W., 2014. Biosens. Bioelectron. 62, 331–336.
Holm, P.I., Ueland, P.M., Kvalheim, G., Lien, E.A., 2003. Clin. Chem. 49 (2), 286–294.
Janssen-Heininger, Y.M.W., Mossman, B.T., Heintz, N.H., Forman, H.J., Kalyanaraman, B., Finkel, T., Stamler, J.S., Rhee, S.G., van der Vliet, A., 2008. Free Radic. Biol. Med. 45 (1), 1–17.
Kazmierczak, M., Wysocki, H., Wykretowicz, A., Minczykowski, A., 1995. Coron. Artery Dis. 6 (1), 65–69.
Kim, G.J., Fiskum, G.M., Morgan, W.F., 2006. Cancer Res. 66 (21).
Kim, H.Y., Ahn, J.K., Park, K.S., Park, H.G., 2020a. Sensor. Actuator. B Chem. 310, 127808.
Kim, H.Y., Lee, C.Y., Kim, H., Park, K.S., Park, H.G., 2020b. Analyst 145 (16), 5578–5583.
Kim, H.Y., Park, K.S., Park, H.G., 2020c. Theranostics 10 (10), 4507–4514.
Kim, H.Y., Song, J., Park, K.S., Park, H.G., 2020d. Chem. Commun. 56 (63), 8912–8915.
Lan, T., Zhang, J., Lu, Y., 2016. Biotechnol. Adv. 34 (3), 331–341.
Machado, L.E.S.F., Shen, T.L., Page, R., Peti, W., 2017. J. Biol. Chem. 292 (21), 8786–8796.
Mahdi, M.A., Yousefi, S.R., Jasim, L.S., Salavati-Niasari, M., 2022. Int. J. Hydrogen Energy 47 (31), 14319–14330.
Meitzler, J.L., Konaté, M.M., Doroshow, J.H., 2019. Arch. Biochem. Biophys. 675, 108076.
Meng, F.G., Zhang, Z.Y., 2013. Biochim. Biophys. Acta Protein Proteonomics 1834 (1), 464–469.
Mohammadniaei, M., Yoon, J., Lee, T., Bharate, B.G., Jo, J., Lee, D., Choi, J.-W., 2018. Small 14 (16), 1703970.
Mohanty, J.G., Jaffe, J.S., Schulman, E.S., Raible, D.G., 1997. J. Immunol. Methods 202 (2), 133–141.
Östman, A., Frijhoff, J., Sandin, Å., Böhmer, F.D., 2011. J. Biochem. 150 (4), 345–356.
Panieri, E., Santoro, M.M., 2016. Cell Death Dis. 7, 2253.
Purohit, B., Mahato, K., Kumar, A., Chandra, P., 2019. Microchim. Acta 186 (9).
Rahman, M.M., Alam, M.M., Asiri, A.M., 2019. RSC Adv. 9 (60), 35146–35157.
Ren, m., Dong, D., Xu, Q., Yin, J., Wang, S., Kong, F., 2021. Talanta 234, 122684.
Rhee, S.G., 2006. Science 312 (5782), 1882–1883.
Roberts, C.K., Barnard, R.J., Sindhu, R.K., Jurczak, M., Ehdaie, A., Vaziri, N.D., 2005. J. Appl. Physiol. 98 (1), 203–210.
Stone, J.R., Yang, S., 2006. Antioxidants Redox Signal. 8 (3–4), 243–270.
Sullivan, L.B., Gui, D.Y., Heiden, M.G.V., 2016. Nat. Rev. Cancer 16, 680–693.
Srinivasan, S., Guha, M., Kashina, A., Avadhani, N.G., 2017. Biochim. Biophys. Acta Bioenerg. 1858 (8), 602–614.
Summers, F.A., Zhao, B., Ganini, D., Mason, R.P., 2013. Methods in Enzymology, pp. 1–17.
Tanner, J.J., Parsons, Z.D., Cummings, A.H., Zhou, H., Gates, K.S., 2011. Antioxidants Redox Signal. 15 (1), 77–97.
Tian, T., Zhang, H., Yang, F.-Q., 2022. Enzyme and Microbial Technology, 110096.
Tripathi, R.M., Chung, S.J., 2020. Molecules 25 (15).
Veal, E.A., Day, A.M., Morgan, B.A., 2007. Mol. Cell 26 (1), 1–14.
Wang, N., Miller, C.J., Wang, P., Waite, T.D., 2017. Anal. Chim. Acta 963, 61–67.

Wierusz-Wysocka, B., Wysocki, H., Byks, H., Zozulińska, D., Wykrętowicz, A., Kaźmierczak, M., 1995. Diabetes Res. Clin. Pract. 27 (3), 193–197.
Wu, P., Cai, Z., Gao, Y., Zhang, H., Cai, C., 2011. Chem. Commun. 47, 11327–11329.
Wu, T., Yang, Y., Cao, Y., Song, Y., Xu, L.P., Zhang, X., Wang, S., 2018. ACS Appl. Mater. Interfaces 10 (49), 42050–42057.
Xiang, Y., Lu, Y., 2011. Nat. Chem. 3 (9), 697–703.
Xiang, Y., Lu, Y., 2012a. Anal. Chem. 84 (9), 4174–4178.
Xiang, Y., Lu, Y., 2012b. Anal. Chem. 84 (4), 1975–1980.
Yousefi, S.R., Alshamsi, H.A., Amiri, O., Salavati-Niasari, M., 2021a. J. Mol. Liq. 337, 116405.
Yousefi, S.R., Amiri, O., Salavati-Niasari, M., 2019a. Ultrason. Sonochem. 58, 104619.
Yousefi, S.R., Ghanbari, D., Salavati-Niasari, M., Hassanpour, M., 2016. J. Mater. Sci. Mater. Electron. 27 (2), 1244–1253.
Yousefi, S.R., Ghanbari, M., Amiri, O., Marzhoseyni, Z., Mehdizadeh, P., Hajizadeh-Oghaz, M., Salavati-Niasari, M., 2021b. J. Am. Ceram. Soc. 104 (7), 2952–2965.
Yousefi, S.R., Masjedi-Arani, M., Morassaei, M.S., Salavati-Niasari, M., Moayedi, H., 2019b. Int. J. Hydrogen Energy 44 (43), 24005–24016.
Yousefi, S.R., Sobhani, A., Alshamsi, H.A., Salavati-Niasari, M., 2021c. RSC Adv. 11 (19), 11500–11512.
Yousefi, S.R., Sobhani, A., Salavati-Niasari, M., 2017. Adv. Powder Technol. 28 (4), 1258–1262.
Zhang, H., Gong, Z.-M., Li, Y., Yang, F.-Q., 2022. Enzym. Microb. Technol. 155, 109996.
Zhang, J., Lan, T., Lu, Y., 2020. TrAC, Trends Anal. Chem. 124.
Zhang, J., Xiang, Y., Wang, M., Basu, A., Lu, Y., 2016. Angew. Chem. Int. Ed. 55 (2), 732–736.
Zhu, X., Sarwar, M., Zhu, J.J., Zhang, C., Kaushik, A., Li, C.Z., 2019. Biosens. Bioelectron. 126, 690–696.